Atmósfera (1994), **7**, pp. 61-74

Changes of sea–air interaction parameters at both sides of the Panama Canal and at the equatorial East Pacific

A. KAPALA, H. MÄCHEL, H. FLOHN

Meteorological Institute, University of Bonn, Germany

(Manuscript received October 21, 1992; accepted in final form July 28, 1993)

RESUMEN

Este trabajo se inserta dentro del marco de nuestros estudios previos que han tratado de cambios recientes en los parámetros atmósfera–océano y de la evaporación sobre los mares tropicales. Esta vez basados en tres secciones elegidas – las áreas en ambos lados del Canal de Panamá y alrededor de las Islas Galápagos – haremos una comparación regional entre las áreas de surgencias contra las áreas oceánicas "calientes", respecto a la variabilidad de los parámetros aire–mar, seleccionados para el periodo 1947-1989.

Se examinaron las tendencias estacionales y anuales; los cambios de promedios década a década, y la variabilidad y la frecuencia relativa de las anomalías de temperatura de la superficie del mar.

Más aún investigamos la correlación entre los parámetros individuales y las conexiones entre las secciones mencionadas. Fuimos capaces de confirmar diferencias temporales y espaciales, razonablemente notables, en los elementos meteorológicos disponibles.

ABSTRACT

This paper complies within the framework of our earlier studies which have dealt with recent changes of sea–air parameters and evaporation over tropical oceans. Here, based on three chosen sections – the areas on both sides of the Panama Canal and around the Galapagos Islands – we will draw a regional comparison between upwelling and "warm" ocean areas with regard to the variability of the selected sea–air parameters in the period 1947-1989. We examined the seasonal and annual trends, decade–to–decade changes of the averages, and the variability and relative frequency of the sea surface temperature's anomalies. Furthermore, we investigated the correlation between the individual parameters and connections between the named sections. We were able to confirm reasonably notable temporal and spatial differences in available meteorological elements.

Introduction

This paper links up with our earlier research whereby we attempted to ascertain the evaporation over the tropical oceans and its changes by investigating the sea–air parameter's variability (Flohn and Kapala, 1989). Based on these studies, as well as bearing in mind the estimation of precipitable water changes over the tropical Pacific (Hense *et al.*, 1988), we tried to deduce the changes of the hydrological cycle (Flohn *et al.*, 1992). Although the essential role of water vapour – the most important greenhouse gas – and its phase changes for the climate system has already been emphasized by several authors (e.g., Möller, 1963; Ramanathan, 1981; Raval and Ramanathan, 1989), nonetheless, relatively few have ventured a detailed examination to date. With regard to the General Circulation Models, measures are only now being taken for more accurate calculations of the hydrological cycle changes (Randall *et al.*, 1992). The difficulties encountered in evaluating the evaporation and the latent heat fluxes respectively based on available records will not be further discussed at this time; this problem has already

been referred to by many other authors (e.g., Kaufeld, 1981; Isemer and Hasse, 1987, 1991; Ramage, 1987; Cardone and Greenwood, 1990).

Investigations of the tropical marine boundary layer have indicated that a weak, regionally varying rise of the sea surface temperature (T_s) was accompanied by a substantial increase of evaporation (E). This is apparently related to a surprisingly large intensification of the mid-latitude atmospheric circulation concentrated above the northern Pacific and the northern Atlantic (Flohn *et al.*, 1990a, b; Nitta and Yamada, 1989). Furthermore, this appears to have been largely due to a 10–20% rise of atmospheric water vapour in the Tropics (Hense *et al.*, 1988). This has, however led to an intensification of ascending motions and rainfall in cyclonic eddies, compensated by higher subsidence in all other regions, notably in the subtropical anticyclonic belt.

Our comparative studies in 32 selected fields – extended along the main shipping routes in the intertropical zone (Lat. 10°S–14°N) – showed remarkable spatial variations of T_s and other parameters at the sea–air interface. The greatest contrasts appear between the upwelling regions in all three oceans and the large area of "warmest oceans" extending from Long. 62°E to the date line. In the latter area – where no large-scale upwelling occurs – the annual average sea surface temperature climbs to 28°C, and in some places to even 29°C. Accompanying the rise of sea–air temperature difference ($T_s - T_a$), high values of the saturation deficit ($q_s - q_a$) lead to a significant rise of evaporation (E), even when assuming a detrended wind speed (V_{scal}). In contrast, the increase of evaporation in the upwelling areas is generally slight, whereas the fluctuation of the saturation deficit and the evaporation, when comparing El Niño to La Niña events, are indeed considerable; the evaporation during warm events increases by several times (Philander, 1989).

Inspection of available data sources suggest that maritime climatological averages vary substantially in the ocean areas at both entrances to the Panama Canal (Fig. 1).

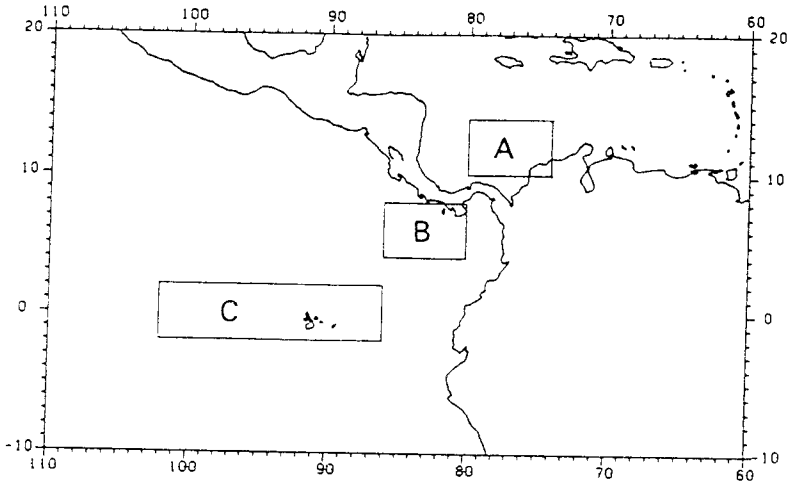

Fig. 1. The geographic location of the investigated oceans sections.

Within the climatically highly differentiated Panama and Galapagos region, three sections along the main shipping routes distinguished by the availability of a large number of meteorological observations were chosen: the section north of the Panama Canal (A) includes six $2^\circ \times 2^\circ$ boxes (10–14°N, 74–80°W) with a total of 149 032 T_s observations (1947-1989) and the section to the south of the Panama Canal (B) six $2^\circ \times 2^\circ$ boxes (4–8°N, 80–86°W), with 107 639 observations. The Galapagos region (section C) covers a part of the equatorial upwelling-area with sixteen $2^\circ \times 2^\circ$ boxes (2°N–2°S, 86–102°W) and approximately 49 062

observations. These areas show various climatic peculiarities caused by the separating effect of the Panama Isthmus.

Taking the Panama and Galapagos regions –here a relatively small part of the equatorial zone totalling 1.4×10^6 km^2 – as an example, the changes of the most important air–sea parameters during the period 1947-1989 should come under closer investigation based upon the maritime observational data COADS. In order to distinguish the climatic conditions and their long–term variations, we examined: annual and seasonal averages, monthly deviations from mean annual cycle (1947-1989) and their linear trends, differences of the decadal mean values as well as the time and space correlations between the monthly normalized anomalies of the sea–air parameters. Normalization is achieved by taking the difference between raw and long–term monthly mean data, expressed in units of standard deviation for the period 1947-1989 at each section.

Annual variations of the sea–air interaction parameters

The averages of the parameters show strikingly different values and annual cycles on both sides of the Panama Isthmus (Fig. 2).

The greatest differences between the three selected areas appear in the *wind conditions*. Section A on the north side of the Panama Canal is characterized by a constant ENE–trade wind with highest velocities occurring during the winter months, with a secondary peak in July. During the summer months, the wind turns slightly towards the east, while the minimum wind velocity is reached in October. In contrast to the area at the northern entrance of the Panama Canal, the existing lee vortex in Section B clearly shows more variable and weaker winds with a resultant NE wind component only during the boreal winter. In April, the wind turns to the south with the SE–trade wind penetrating into the Northern Hemisphere. During the summer, the wind direction changes to WSW and increases in velocity. The Galapagos section (C) remains within the SE–trades zone (with southerly directions dominating) throughout the entire year. A weak SSE-wind prevails during May and June. The considerable – both regional and seasonal – variations of the mean wind velocities are reflected in the relatively low correlation coefficients of the monthly anomalies of the scalar wind speed (V_{scal}) between these sections.

The *sea surface temperature* (T_s) in the areas at the northern and southern entrance of the Panama Canal show very similar long–term annual averages of 27.67 and 27.66°C, respectively (Table 1). There is, however, a definite contrast in the annual variations. In Section A, T_s reaches its maximum of 28.75°C in October and its minimum of 26.44°C in February, and follows the typical annual cycles of the Northern Hemisphere's subtropical regions. Section B attains its highest (28.33°C) T_s in April and its lowest (27.12°C) in November. Distinctively lower T_s can be observed in the equatorial upwelling Section C; with an annual mean of 24.34°C, T_s varies here between 26.73°C in March and 22.70°C in September, with an annual amplitude reaching 4°C.

The *sea–air temperature difference* ($T_s - T_a$) shows positive annual mean values in all areas between 1947-1989. In both Pacific fields it is distinctively higher than in Section A, where the maxima occur during autumn (Sept.–Oct.) and the minima in spring (March–April). The monthly sea–air temperature difference partially takes on negative or high positive values and is related to El Niño events.

The *saturation deficit* ($q_s - q_a$) for the annual mean (1947-1989) in the areas on both sides of the Panama Canal reaches more than 4 g/kg, while in the equatorial (upwelling) Section C, it drops to values around 3.4 g/kg – in accordance with the prevailing relatively low sea and air temperatures. In the spring, while a maximum is reached in Section B, a minimum is reached

in Section A, whereas both a spring and autumn maximum is observed in Section C. Here the year-to-year fluctuations are remarkable. The mean annual cycle (1947-1989) of $q_s - q_a$ reflects slight shifts of sea and air temperature.

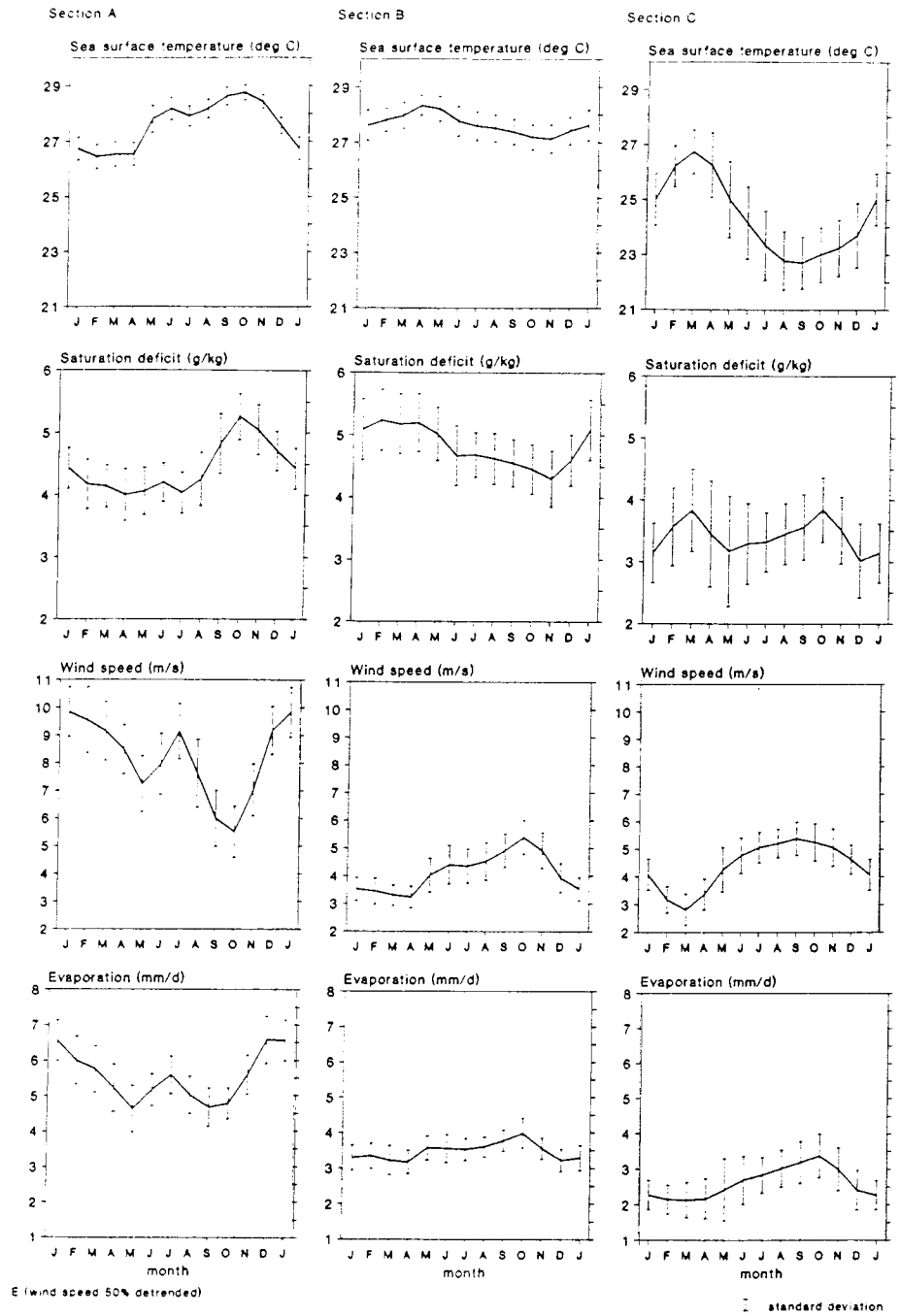

Fig. 2. Annual variations and standard deviation of sea surface temperature (T_s), saturation deficit ($q_s - q_a$) scalar wind speed (V_{scal}) and evaporation (E_{50} with 50% detrended wind speed) for Sections, A, B and C in the period 1947-1989.

In all sections, *relative humidity* (RH) clearly reaches more than 80%, with little seasonal fluctuations. The annual variations in RH, especially in Section B, are apparently influenced by wind conditions. On the lee side of the NNW to ENE winds, relative humidity decreases to values around 80%.

Tendencies in the long–term variations of the sea–air parameters

The interannual variations of the sea–air interface parameter and changes in the period 1947-1989 will be dealt with in this chapter. The variations of the most important sea–air parameter for the annual means and the extreme seasons (January–April and July–October) in the period 1947-1989 are visualized in Table 1 using tertials.

Table 1: Averages of the sea-air interface parameters 1947-1989

	1-4	7-10	Year	1-4	7-10	Year	1-4	7-10	Year
	T_s (°C)			T_s-T_a (°C)			RH (%)		
Section A	26.67	28.36	27.67	0.15	0.39	0.30	81.69	83.06	82.49
Section B	27.93	27.41	27.66	0.51	1.28	0.95	80.59	86.41	84.09
Section C	26.03	22.95	24.34	0.35	0.98	0.62	85.38	84.71	85.14
	q_s-q_a (g/kg)			V_{scal} (m/s), corr.			E_{50} mm/d		
Section A	4.19	4.59	4.43	10.65	8.47	9.46	5.88	5.00	5.46
Section B	5.18	4.57	4.80	4.75	6.20	5.56	3.26	3.72	3.49
Section C	3.50	3.54	3.43	4.74	6.63	5.82	2.18	3.11	2.64

Initially, analysis of the linear trend was used in identifying the long–term changes of the previously mentioned parameters. In doing so, the existence of trends significantly different from zero was examined by means of the t–test. The t–test has been applied to each of the regression lines (dependant variables: for example T_s anomalies) as a function of months.

Table 2: Linear trends of the sea-air interface parameters 1947-1989

	1-4	7-10	Year	1-4	7-10	Year	1-4	7-10	Year
	T_s (°C)			T_s-T_a (°C)			RH(%)		
Section A	+.28	-.18	+.03	-.07	-.17 **	-.12 **	-1.05 *	-1.38 ****	-1.34 ****
Section B	+.08	+.14	-.17	-.20 **	-.18 **	-.19 ****	-.24	-1.55 ***	-1.02 ***
Section C	+.17	+.43	+.40	-.40 ***	-.62 ****	-.48 ****	-.56	-2.35 ****	-1.46 ***
	q_s-q_a (g/kg)			V_{scal}			E_{50} (mm/d)		
Section A	+.21	+.07	-.17	+.67 **	+1.77 ****	+1.22 ****	+.49 **	+.60 ****	-.57 ****
Section B	-.13	-.09	-.06	+.72 ****	+.82 ***	+.71 ****	+.10 *	+.30 ***	-.27 ****
Section C	-.27	-.08	-.08	+.57 ***	+1.05 ****	+.80 ****	-.02	-.20	-.15

Significance level: **** 99.9% *** 99.0% ** 95.0% * 90.0%

The results of this investigation are compiled in Table 2. Figure 3 clearly shows the long-term changes in the monthly anomalies of the selected parameters. The values in Table 2 illustrate that the magnitude of the estimated trends as well as their significance suggest remarkable seasonal and regional changes in the researched parameters.

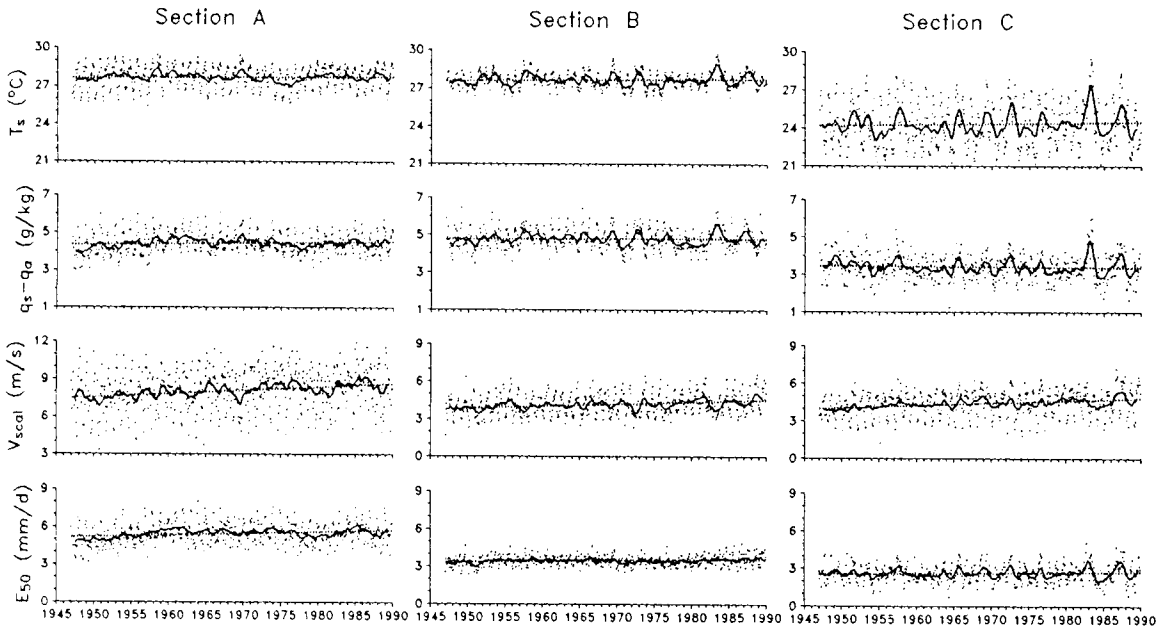

Fig. 3. Long-term variations of the monthly anomalies (points) of sea surface temperature (T_s), saturation deficit ($q_s - q_a$), scalar wind speed (V_{scal}) and evaporation (E_{50} with 50% detrended wind speed) for Sections A, B and C. Smoothed line: the 13-point low-pass Gaussian filter; dashed line: linear trend for the period 1947-1989.

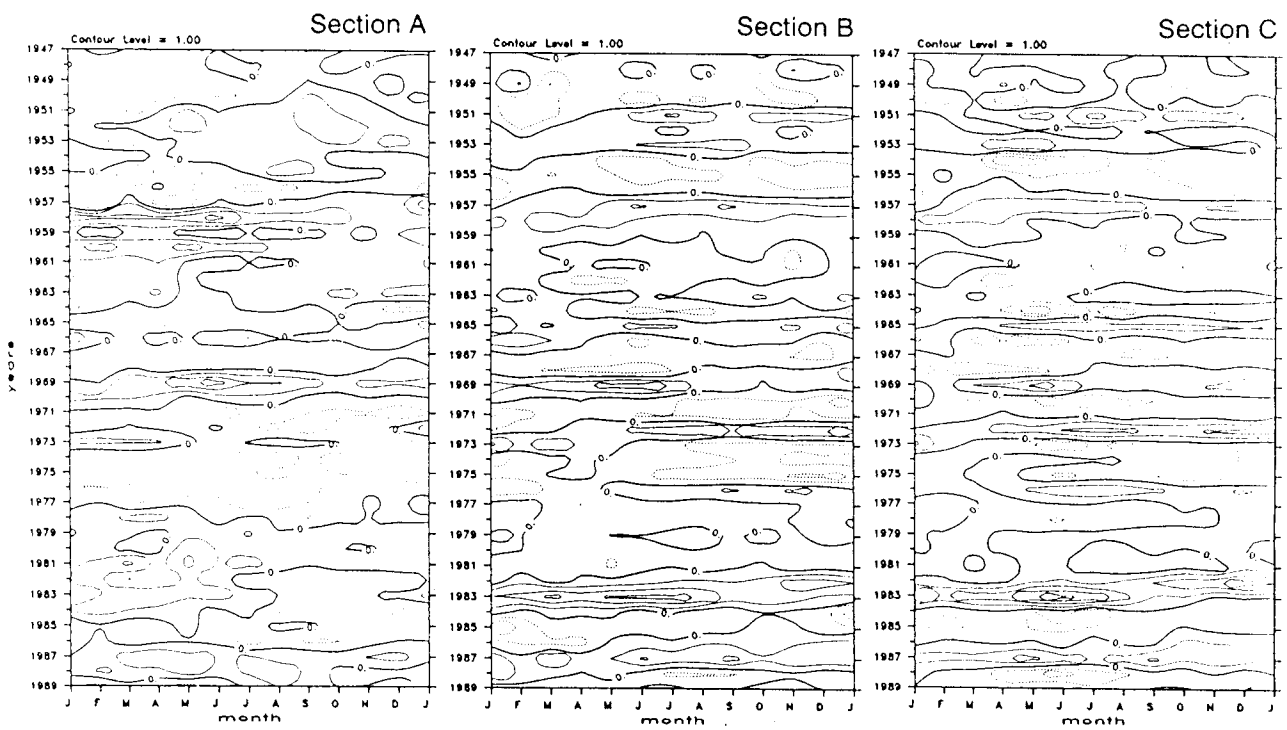

Fig. 4. Standardized monthly anomalies of the sea surface temperature (T_s) in the period 1947-1989 for Sections A, B and C; dashed line: negative anomalies.

In the period 1947-1989, remarkable changes of sea surface temperature (T_s) were observed in all three sections. While a slight decrease in T_s was realized in Section A during July through October, there was an increase in the other sections. Nevertheless, the calculated linear trends are not significant. This is a result of the strong annual and interannual variabilities of T_s, especially in the equatorial upwelling area (C), where the highest rise of T_s is observed. This rise is related to a greater frequency of the extremely high positive anomalies during the 80's (Fig. 5).

Henceforth, we would like to consider the interannual and monthly variability of the T_s anomalies (standardized) respectively. Figures 4a-c contain the monthly distributions of the T_s anomalies in standard deviation units. These figures reveal not only that the frequencies but also that the timespan of high positive T_s anomalies have risen since the 70's. This has been most notably observed in Section C. Here, in comparison with the period 1950-1959, the intensity as well as the duration of the extremely strong El Niño events has been extended. The highest positive T_s anomalies ever were recorded during the 1982/83 El Niño. A similar distribution of T_s patterns could be observed in Section B. In this case, the intensity and the duration of the El Niño events is nevertheless clearly weaker and short-lived. It is, however, remarkable that the negative T_s anomalies were more concentrated during the 70's. This is most prominently apparent within Section A, even though the distribution of the T_s anomalies here show a somewhat lesser marked pattern than in the other two areas.

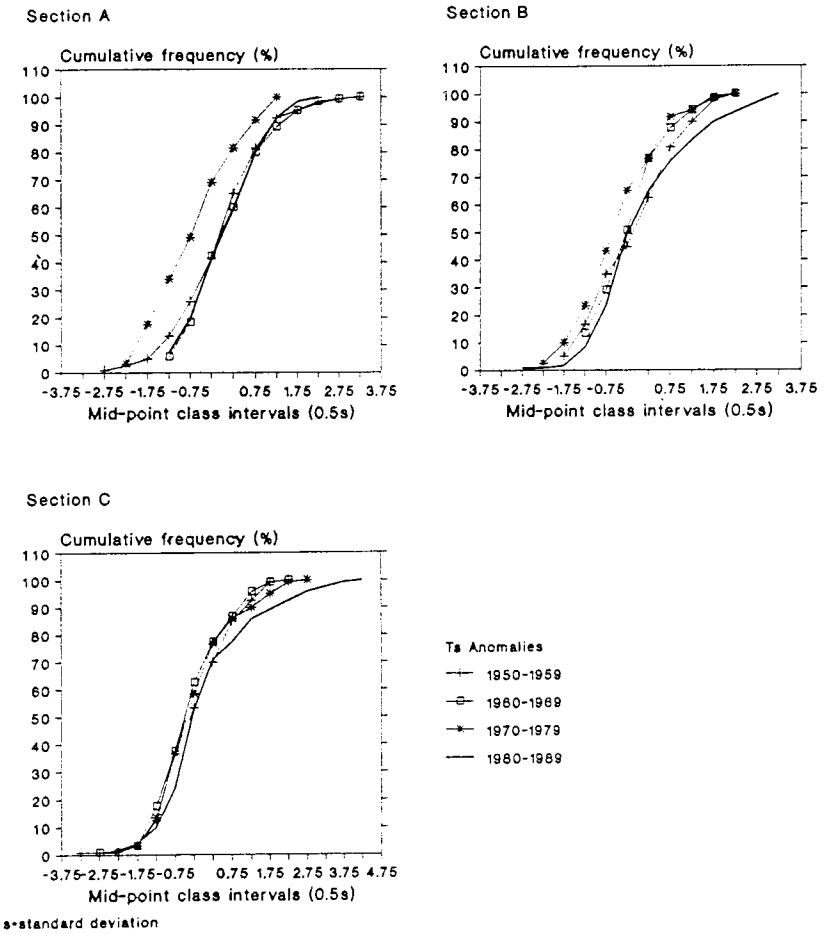

Fig. 5. Comulative relative frequencies of the standardized monthly sea surface temperature in the periods 1950-1959, 1960-1969, 1970-1979 and 1980-1989 for Sections A, B and C.

In addition to the estimation of the monthly anomalies linear trends of the individual parameters over the entire period 1947-1989, the averages in the decades 1950-1959, 1960-1969, 1970-1979 and 1980-1989 (each containing 12 monthly means) were compared and cross-checked as to whether these means were significantly different. Table 3 shows the decade-to-decade differences of the mean values in the selected paramenters. With the exception of the significant increase of T_s mean values in all three sections during the 80's in relation to the 70's, the deviations of the values resulting after comparing pairs of the specific periods reveal no clear-cut pattern of changes in the parameters. In Sections A and B, the average of T_s was significantly lower during the 70's than during the 60's. The saturation deficit ($q_s - q_a$) means of these two areas show a similar tendency. Furthermore, striking differences also appear in V_{scal} mean values, most notably – although not significant – between the periods 1960-1969 and 1950-1959. This could possibly be due to the fact that changes from estimation to measurement of wind speed primarily took place during these decades (Ramage, 1987); the increase of mean values during the 70's in relation to the 80's is minute. The exception here is Section A, where, contrary to the 60's, a significant increase in V_{scal} mean values during the 70's was recorded, although when compared to the timespan 1980-1989, the wind speed hardly increased at all. In contrast to this, a marked enhancement of V_{scal} was observed in Sections C and A. Apparently this increase in V_{scal} mean values during the 80's can hardly be attributed to the gradual transition from wind estimates based on sea-state to anemometer measurements. It may therefore be surmised that the existing strong linear trends found in the wind reports of COADS-data are partly real.

Table 3: Decade-to-decade changes of the arithmetic means of the sea-air interface parameters

	T_s	$q_s - q_a$	V_{scal}	E_{50}
Section A				
Δ x 1960/69-1950/59	+0.070	+0.250	+0.238	+0.372
Δ x 1970/79-1960/69	-0.292	-0.216	-0.461	-0.081
Δ x 1980/89-1970/79	+0.276	+0.055	+0.078	+0.042
Section B				
Δ x 1960/69-1950/59	-0.035	+0.053	+0.216	+0.115
Δ x 1970/79-1960/69	-0.146	-0.169	+0.057	-0.148
Δ x 1980/89-1970/79	+0.287	+0.135	-0.265	+0.230
Section C				
Δ x 1960/69-1950/59	-0.121	-0.104	+0.158	+0.020
Δ x 1970/79-1960/69	-0.213	-0.007	+0.013	-0.038
Δ x 1980/89-1970/79	+0.308	+0.129	+0.223	+0.155

Remark: Significant differences at 95% level underlined

Hence, we attempted to closely examine the frequency of the monthly anomalies within the same decade, similar to the comparison of the mean values (for the mean annual cycle and the standard deviation the reference period is 1947-1989). According to the Chi^2-test only for both Pacific sections in 1980-1989 and for Section A in 1970-1979, the frequency of these monthly anomalies within the separate decades (120 months each) and regions showed significant deviation in comparison with the standard-normal distribution. As can be seen by the frequency of the T_s anomalies (not shown) and the slightly increased skewness from decade-to-decade – for example, in Section C – there was a remarkable shifting to extremely high positive anomalies,

especially during the 80's. The relative cumulative frequency of anomalies in the separate decades compiled in Figure 5, clearly reflects the regional as well as the temporal changes in the behaviour of the T_s anomalies. Most notable are the significant differences in Section A, where, in comparison with the other decades, a marked shift to the negative anomalies took place during the 70's. According to the Kolmogorov–Smirnov test, the difference in the frequency of T_s anomalies between the 70's and the 80's is significant at the 95% level.

Most remarkable is the strong decline of the *difference between sea and air temperature* $(T_s - T_a)$ which is significant almost everywhere, especially in Section C. In this section, there was a 41% decline in July through October, and a 77% decline in the annual average in relationship to the long–term mean. Furthermore, as observed in the other sections, the air temperature increased much stronger than that of the sea.

Changes in the *saturation deficit* $(q_s - q_a)$ show varied but insignificant linear trends. In contrast to the observed increase in the Atlantic section, there was a decrease in both Pacific sections.

The greatest changes can be observed in the *wind conditions*. In Section A, the wind's northerly and especially easterly components (ENE trades) were notably stronger in the summer/autumn than in the spring (with nearly persistent wind steadiness, as derived from monthly averages). In Section B, the southerly and westerly components intensified, with the westerly component more dominant in the spring and the southerly component more so in the summer/autumn (likewise with nearly persistent wind steadiness). Although to a lesser degree, a marked increase (more than 95% significant) of the easterly as well as of the southerly component has been noted in Section C. Secion A shows the strongest intensification of wind speed for the annual means during the period 1947-1989, concentrating especially on the summer/autumn months. A similar development is visible in Section B, although here the trends are distinctively lower. Section C also shows the largest, most significant increase of wind speed in the summer/autumn, while only a relatively low trend appears during the spring.

These comparisons have made clear that the individual sea–air parameters show relatively large temporal and regional variations so that a similar differentiation in evaporation can be anticipated.

Evaluation of evaporation and its variation

Based on available, although in part inaccurate, data only a rough estimate can be given instead of the exact value of oceanic evaporation (E). In this case, we are primarily concerned about the time changes. The estimation of monthly means of oceanic evaporation (E in mm per day) is based on the standard bulk formula:

$$E = \rho c_E (q_s - q_a) V_{scal}$$

Here q_a and q_s represent the specific humidities (in g/kg) of the air and the saturation value at the temperature of the sea surface, respectively; ρ is the air density, which is used as constant, with value $\rho = 1.173$ kg/m^3, and c_E is the bulk transfer coefficient for water vapour, here with 1.3×10^{-3}. For discussion see Isemer and Hasse (1987).

As in our previous investigations, the monthly mean value of V_{scal} (from COADS data which have been converted into metric units using an outdated table) was corrected by +1.4 m/s. This correction (only for tropical areas) was calculated according to Kuhlbrodt's (1936) data for Beaufort force 1–6.

Considering the inhomogeneities of wind reports caused by the applied measuring techniques (transition from estimate to measurement), a too high, unrealistic trend in V_{sc} is assumed. Consequently, the estimate of the evaporation variations for the period 1947-1989 is proposed in three versions: a) assuming detrended V_{scal} values (E_0), b) original not detrended V_{scal} values (E_{100}), and c) 50% detrended V_{scal} value (E_{50}).

The estimated evaporation resulting under the assumption of 50% of the calculated V_{scal} linear trend amounts to 5.46 mm/d in the Section A, 3.49 mm/d in B and 2.64 mm/d in the upwelling region C (Tab. 2); this is equivalent to an average annual evaporation of 1993 mm, 1274 mm and 964 mm. In terms of energy flux units this translates into 154 W/m^2, 98 W/m^2 and 74 W/m^2, respectively.

In Section A, the maximum of evaporation falls on the winter months during which time the wind reaches its highest velocity (Fig. 2). The second annual minimum occurs during autumn, accompanied by a minimum of wind speed and a maximum of the saturation deficit. In both Pacific sections, the annual fluctuation of evaporation is notably smaller, with a maximum reached in the boreal summer. The higher rate of evaporation in Section B is associated with a maximum of wind velocity and a minimum of the saturation deficit, while in Section C, the highest rate of evaporation coincides with the second annual maximum of saturation deficit. To a varying degree in the individual regions, the annual cycle of evaporation is influenced as a consequence of the partly opposed variations of V_{scal} and $q_s - q_a$.

With regard to the linear trends, examination of the long-term variations of E gives the following results:

Had there been no change in scalar wind speed during the period examined, the areas on both sides of the Panama Canal would have shown an evaporation increase in the annual means between 1.1% and 3.8%. Accounting for the full linear trend of scalar wind speed, there would be an increase of annual means of E around 14% (Section B) and 17% (Section A). These values vary between 14% and 13% in the winter/spring as well as 14% and 29.3% during the summer/autumn. Both extreme suppositions appear to be unrealistic and only suggest possible limitations for further more realistic assumptions. As in our previous publications, we allowed for 50% of the scalar wind speed trend in estimating evaporation (E_{50}).

Accordingly, our calculations yield an increase of annual evaporation (E_{50}) of around 10% for Secction A, in the spring (summer/autumn) of around 9% (12%). The area south of the Panama Canal (B) shows a lower annual increase of 7.4% because of the partly opposite trends of $q_s - q_a$ and V_{scal}. Due to contrary trends of $q_s - q_a$ and V_{scal} in the Galapagos region (C), only a slight increase of evaporation is noted; during the spring the trend is very small and in autumn it is indeed greater, while not significantly different from zero (Table 2).

These results indicate a distinct regional variability of recent trends of the ocean–atmosphere flux and require further detailed investigation. The markedly different trends of V_{scal} at both sides of the Panama Isthmus also reflect the partial reality of the global V_{scal} rise after the Second World War, bearing in mind that all observations in Section B are made on the same ships contributing 72% of observations in Section A.

Table 4 contains the correlation coefficients for the sea–air parameters in the three areas examined. A comparison of Sections A and C show striking differences. No connection exists between E_{50} and T_s in the area of the study NE–trade wind (A) and E_{50} here correlates highly with V_{scal}. In the eastern Pacific upwelling region, the evaporation (E_{50}) showed the highest correlation with $q_s - q_a$ and T_s. Here, the connection between E_{50} and V_{scal} is slightly lower.

The various seasonal changes, especially in the Galapagos region, indicate irregular El–Niño events which primarily occur during the boreal winter months. These seasonal changes are

related to the advance of warm sea-surface water in upwelling regions which in turn intensifies evaporation by a factor up tc 4. During El Niño events, not only does the evaporation, and consequently the water vapour content in the troposphere, increase remarkably, but the warming of the sea surface is also accompanied by an enhancement of a CO_2-flux into the atmosphere (Elliot and Angell, 1987).

Table 4: Correlations of the sea-air interface parameters (monthly anomalies)

	T_s	T_s-T_a	q_s-q_a	RH	u-comp.	v-comp.	V_{scal}
Section A							
T_s-T_a	+.381						
q_s-q_a	+.486	+.664					
RH	-.012	+.005	-.703				
u-comp.	+.435	+.463	+.357	+.032			
v-comp.	+.402	+.456	+.339	+.040	+.684		
V_{scal}	-.448	-.448	-.326	-.067	-.952	-.760	
E_{50}	-.055	+.076	+.417	-.559	-.649	-.480	+.691
Section B							
T_s-T_a	+.199						
q_s-q_a	+.716	+.426					
RH	-.378	+.297	-.696				
u-comp.	-.513	+.069	-.511	+.518			
v-comp.	-.464	+.079	-.492	+.516	+.642		
V_{scal}	-.448	-.117	-.392	+.248	+.643	+.591	
E_{50}	+.191	+.328	+.499	-.325	+.155	+.132	+.573
Section C							
T_s-T_a	+.159						
q_s-q_a	+.753	+.570					
RH	-.496	+.120	-.673				
u-comp.	-.025	+.267	+.134	+.055			
v-comp.	+.290	-.068	+.170	-.210	-.197		
V_{scal}	+.365	-.147	+.222	-.325	-.424	+.880	
E_{50}	+.762	+.397	+.882	-.661	-.074	+.550	+.624
	T_s	T_s-T_a	q_s-q_a	RH	u-comp.	v-comp.	V_{scal}

Remark: correlation coefficients significant at 95% level are underlined

Table 5: Correlation between the sections (monthly anomalies)

Section	T_s	T_s-T_a	q_s-q_a	RH	V_{scal}	E_{50}
A/B	+.333	+.195	+.023	+.237	-.103	+.134
A/C	+.124	+.106	+.119	+.008	+.143	-.125
B/C	+.740	+.178	+.393	+.349	+.039	+.067

Remark: correlation coefficients significant at 95% level are underlined

The correlation coefficient between T_s, $q_s - q_a$, and (to a weaker degree) $T_s - T_a$ are positive and significant everywhere. A strong negative correlation exists between RH and $q_s - q_a$; we are unfortunately not able to provide a physical interpretation of the significantly negative (annual) trend of RH.

With regard to the changes of the examined parameter, the spatial connection between the sections is as follows;

A highly statistically significant correlation ($r = +.740$) exists between the monthly-anomalies (over all 516 months) of T_s in both Pacific sections. As expected, a distinctively lower correlation can be found in the sections on both sides of the Panama Canal ($r = +.333$); the simultaneous T_s anomaly observed in Section B is only perceptible 5 months later in Section A ($r = +.477$).

The correlation of the $T_s - T_a$ monthly anomalies between the Sections B and A is statistically significant and higher than between Sections C and B. A highly significant correlation of the monthly anomalies of $q_s - q_a$ exists only between Sections B and C. The RH's monthly anomalies show a 99.9% significant correlation in Sections B/A and B/C respectively whereas the Sections A/C show no significant relationships.

Concluding remarks

With respect to changes of the sea–air parameters within the period investigated (1947-1989), the following can be summarized:

The linear trends of T_s are not significant, however, relative humidity decreases in the annual average and in the summer/autumn in all sections. Intensified wind speed in both trade zones (especially during the northern summer/southern winter) is temporally and spatially different and therefore this trend appears, at least in part, to be real. The humidity gradient, which according to the high correlation coefficient is decisive for increased evaporation, increases only slightly over the entire year in the NE–trade. Together with the increased wind speed it results, nevertheless, in a considerable enhancement to the already high evaporation rate. The specific humidity difference decreases in both Pacific areas in annual and spring averages. This is obviously related to the (partly real) significant increase of wind speed. Consequently, the increase in evaporation is low, as compared to our results in the warmest oceans in the western tropical Pacific (Flohn *et al.*, 1992). It is near zero in the vicinity of the equator during winter. In the equatorial upwelling Section (C), the correlation between T_s and E is considerably higher than in Section B. In contrast, this correlation in Section A is negative due to the prevailing influence of the wind speed.

The estimated increase of evaporation in the areas on both sides of the Panama Canal is similar to that already observed in the warmest oceans (Flohn *et al.*, 1992). Here the E_{50} trends (in energy flux values) in average during the period 1947-1989 are in the order of 7.6 W/m^2 (Section B) to 16 W/m^2 (Section A). In the equatorial upwelling region affected by El Niño events, the periodic fluctuations of evaporation, and of latent heat fluxes respectively, are large. For example, the latent heat flux in Section C was about 60 W/m^2 higher during the strong El Niño event 1982-83 than the mean value of the period 1947-1989.

Even when considering that 50% of the observed wind speed trend is taken into account, the energy input into the atmosphere via oceanic evaporation is more than 4 times higher than the additional greenhouse effect which results in an increased content of carbon dioxide and other trace gases. According to the IPCC–Report, this effect is about 2 W/m^2 (Houghton *et al.*, 1990).

These results support our previous investigation of the rising water vapour content in the troposphere over the equatorial Pacific (Hense *et al.*, 1988), and do not contradict those of climate models which forecast the highest warming rates for the middle troposphere over tropical areas (Hansen *et al.*, 1984, Wilson and Mitchell, 1987).

Acknowledgement

We particularly thank Mrs. W. Rubin for typing and correcting the English version of this manuscript.

REFERENCES

Cardone, J. and J. G. Greenwood, 1990. On trends in historical marine wind data. *Journ. Climate*, **3**, 113-127

Elliott, W. P. and J. K. Angell, 1987. On the relation between atmospheric CO_2 and equatorial sea–surface temperature. *Tellus*, **39B**, 171-183.

Flohn, H. and A. Kapala, 1989. Changes of tropical sea–air interaction processes over a 30–year period. *Nature*, **338**, 244-246,

Flohn, H., A. Kapala, H.-R. Knoche and H. Mächel, 1990a. Recent changes of tropical water and energy budget and of midlatitude circulations. *Climate Dynamics*, **4**, 237-252.

Flohn, H., A. Kapala, H.-R. Knoche and H. Mächel, 1990b. Changes of hydrological cycle and Northern Hemisphere circulation and their initiation at the tropical air–sea surface. In: Internat. TOGA Scient. Conf. Proceedings, Honolulu 1990, World Meteor. Org. WCRP 43 (WMO/TD 379): 47-57; also in: Houghton J. T. *et al.* (Eds.): Observed Climate Variations and Change: Contributions in Support of Section 7 of the 1990 IPCC Scientific Assessment, Chapter VI:1-11.

Flohn, H., A. Kapala, H.-R. Knoche and H. Mächel, 1992. Water vapour and amplifier of the greenhouse effect: new aspects. *Meteorologische Zeitschrift*, **1**, 122-138.

Hense, A., P. Krahe and H. Flohn, 1988. Recent fluctuations of tropospheric temperature and water vapour content in the Tropics. *Meteor. Atmos. Physics*, **38**, 215-227.

Hansen, J., A. Lacis, D. Rind, G. Russel, P. Stone, I. Fung. R. Ruedy and J. Lerner, 1984. Climate sensitivity: analysis of feedback mechanisms. In: Hansen J. E., T. Takahashi (Eds.): Climate processes and climate sensitivity, Geophys. Monogr. Ser. 29 AGU Washington DC, 130-163.

Houghton, J. T., G. J. Jenkins and J. J. Ephraums (Editors), 1990. Climate Change. The IPCC Scientific Assessment. Cambridge University Press. 365 pp.

Isemer, H.-J. and L. Hasse, 1987. The Bunker Climatic Atlas of the North Atlantic Ocean. Air–Sea Interactions. Vol. 2, Springer Verlag Berlin. 252 pp.

Isemer, H.-J. and L. Hasse, 1991. The scientific Beaufort equivalent scale: Effects on wind statistics and climatological air–sea flux estimates in the North Atlantic Ocean. *Journ. Climate*, **4**, 819-836.

Kaufeld, L., 1981. The development of a new Beaufort equivalent scale. *Meteor. Rundschau*, **34**, 17-23.

Kuhlbrodt, L., 1936. Vergleich geschätzter Windstärken mit gemessenen Windgeschwindigkeiten auf See. *Ann. Hydrogr. Mar. Meteor.*, **64**, 2. Köppen-Heft, 14-23.

Möller, F., 1963. On the influence of changes in the CO_2 concentration in air on the radiation balance of the earth's surface and on the climate. *Journ. Geophys. Res.*, **68**, 3877-3886.

Nitta, T. S. and S. H. Yamada, 1989. Recent warming of tropical sea surface temperature and its relationship to the Northern Hemisphere circulation. *Journ. Meteor. Soc. Japan*, **67**, 375-383.

Philander, S. G. H., 1989. El Niño, La Niña, and Southern Oscillation. In: *International Geophysics Series*, **46**, 293 pp.

Ramage, C. S., 1987. Secular change in reported surface wind speeds over the ocean. *Journ. Clim. Appl. Meteor.*, **26**, 525-528.

Ramanathan, V., 1981. The role of ocean–atmosphere interactions in the CO_2 climate problem. *Journ. Atmos. Sci.*, **38**, 918-930.

Randall, D. A., R. D. Cess, J. P. Blanchet, G. J. Boer, D. A. Dazlich, A. D. Del Genio, M. Deque, V. Dymnikov, V. Galin, S. J. Ghan, A. A. Lacis, H. Le Treut, Z.-X. Li, X.-Z. Liang, B. J. McAvaney, V. P. Meleshko, J. F. B. Mitchell, J.-J. Morcrette, G. L. Potter, L. Rikus, E. Roeckner, J. F. Royer, U. Schlese, D. A. Sheinin, J. Slingo, A. P. Sokolov, K. E. Taylor, W. M. Washington, R. T. Wetherald, I. Yagai and M.-H. Zhang, 1992. Intercomparison and interpretation of surface energy fluxes in Atmospheric General Circulation Models. *Journ. Geophys. Res.*, **97**, 3711-3724

Raval, A. and V. Ramanathan, 1989. Observational determination of the greenhouse effect. *Nature*, **342**, 758-761.

Wilson, C. A. and J. F. B. Mitchell, 1987. A doubled CO_2 climate sensitivity experiment with a global climate model including a simple ocean. *Journ. Geophys. Res.*, **92**, 13315-13343.